The first balloon-borne sample analysis of atmospheric carbonaceous components reveals new insights into formation processes

Roland Benoit, Hazel Vernier, Jean-Paul Vernier, Lilian Joly, Nicolas Dumelié, Frank Wienhold, Cyril Crevoisier, Sandrine Delpeux, François Bernard, Philippe Dagaut, et al.

The first balloon-borne sample analysis of atmospheric carbonaceous components reveals new insights into formation processes

Roland Benoit[1*], Hazel Vernier[2], Jean-Paul Vernier[3, 4], Lilian Joly[5], Nicolas Dumelié[5], Franck G. Wienhold[6], Cyril Crevoisier[7], Sandrine Delpeux[8], Philippe Dagaut[1], Gwenaël Berthet[2].

1 ICARE, UPR 3021, CNRS-INSIS, Orléans, France
2 LPC2E, UMR 7328 CNRS-Université d'Orléans-CNES, Orléans, France
3 NASA Langley Research Center, National Institute of Aerospace, Hampton, VA, USA
4 National Institute of Aerospace, Hampton, VA, USA
5 GSMA, UMR 7331 CNRS-Université de Reims Champagne-Ardenne, Reims, France
6 Federal Institute of Technology (ETHZ), Zurich, Switzerland
7 Laboratoire de Météorologie Dynamique (LMD/IPSL), CNRS, Ecole polytechnique, Université Paris-Saclay, Palaiseau, France
8 ICMN, UMR 7374 CNRS-Université d'Orléans, Orléans, France

* Corresponding author.
E-mail addresses: Roland.benoit@cnrs-orleans.fr

Abstract

Atmospheric aerosol optical, physical, and chemical properties play a fundamental role in the Earth's climate system. A better understanding of the processes involved in their formation, evolution, and interaction with radiation and the water cycle is critical. We report the analysis of atmospheric molecules/particles collected with a new sampling system that can fly under regular weather balloons for the first time. The flight took place on 18/02/2022 from Reims (France). The samples were subsequently analyzed by high-resolution mass spectrometry (Orbitrap) to specifically derive hundreds of organic components present in 4 different layers from the troposphere to the stratosphere (up to 20 km). Additional measurements of O3, CO, and aerosol concentrations a few hours before this flight took place to contextualize the sampling. After separating common species found on each filter that might be common to atmospheric layers or residuals for contaminations, we found that each sample yields significant differences in the number and size of organic species detected that must reflect the unique composition of atmospheric layers. While tropospheric samples yield significantly oxidized and saturated components, with carbon numbers below 30 that might be explained by complex organics chemistry from local and distant source emissions, the upper tropospheric and stratospheric samples were associated with increased carbon numbers (C>30), with a significantly reduced unsaturation number for the stratosphere, that might be induced by strong UV radiations. The multimodal distributions of carbon numbers in chemical formulas observed between 15-20 km suggest that oligomerization and growth of organic molecules may take place in aged air masses of tropical origin that are known to carry organic compounds even several km above the tropopause where their lifetime significantly increases. Overall, these results are consistent with the injection of fire smoke months before the insitu observations and with thermodynamics inherent to conditions prevailing in the stratosphere.

Key words: DESI, Orbitrap, organic aerosols, troposphere, stratosphere

Graphical abstract:

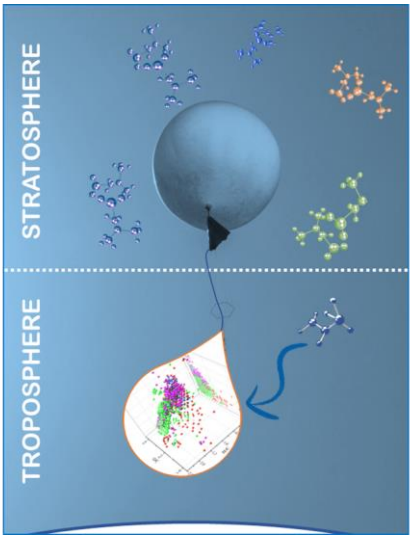

Highlights:

- A new experiment setup was designed and used to chemically characterize organic matter present in the atmosphere (troposphere to the stratosphere)
- We found that each sample collected in different atmospheric layers yields significant differences in terms of the number and size of organic species detected that must reflect the unique composition of atmospheric layers.
- The multimodal distributions of carbon numbers in chemical formulas observed between 15-20 km suggest that oligomerization and growth of organic molecules may take place in aged air masses of tropical origin that are known to carry organic compounds even several km above the tropopause.
- The present results are consistent with the injection of fire smoke months before the in situ observations and with thermodynamics inherent to conditions prevailing in the stratosphere

1. Introduction

Particles in the atmosphere arise from natural sources, such as dust, sea spray, wildfires, and volcanoes, and from anthropogenic activities, such as the combustion of fuels. Primary aerosol particles are emitted directly into the atmosphere and secondary aerosol particles are formed by gas-to-particle conversion processes. They evolve in size and composition through condensation/evaporation of gases, by coagulating with other particles, by chemical reaction, or by activation to become nuclei for liquid or ice clouds formation

Aerosol particles play an important role in the radiative balance of the Earth, with cooling and warming effects depending on particle optical properties according to their size distribution and composition [1]. The export of aerosols and of their precursors from their source areas is associated with atmospheric chemical processes that affect air quality [2] and deplete the stratospheric ozone layer [3]. The aerosol effects depend on the altitude levels but overall are estimated to provide a net negative radiative forcing associated with a cooling of the surface [4]. However, uncertainties in the estimation of aerosol impacts are still large because of the scarcity of observations and the difficulty to characterize the complex aerosol microphysical and chemical properties with respect to altitude.

Tropospheric aerosols contain major fractions of organics (up to 90 %) [5-7]. The oxidation of volatile organic compounds results in the formation of secondary organic aerosols (SOA). A number of studies have been dedicated to the chemical characterization of tropospheric organic aerosol (OA) particles and to the investigation of the physical and chemical pathways for the formation of OA. In particular, reactions of carbonyl-containing organic species, including organosulfate formation and oligomerization reactions have been reported as potential sources of low-volatility organic products in OA [8-10]. Photochemical aging of the light-absorbing OA by photolysis and oxidation by ozone and OH is a significant sink of OA[11].

In the tropics, convective upwelling transports aerosol precursor gases and primary particles from the lower to the upper troposphere [12] where homogeneous nucleation and particle growth processes form secondary particles. Once in the upper troposphere/lower stratosphere (UTLS) region, air masses sustain large-scale transport via the Brewer-Dobson (BD) circulation [13], first upward within the tropical stratosphere and subsequently poleward to descend finally through the lowermost stratosphere into the extratropical troposphere. In addition, direct two-way mass exchange between the upper troposphere (UT) and lowermost stratosphere (LMS), through the extratropical tropopause, occurs along isentropic surfaces. In the stratosphere, the dominant aerosol population consists of droplets of sulfuric acid and water, formed via gas to particle conversion of mainly carbonyl sulfide (OCS) and sulfur dioxide (SO_2) [14]. OCS photo-oxidizes at high altitudes, within the deep BD branch, while SO_2 oxidizes at all altitudes in the stratosphere [15]. In the stratosphere particles are largely submicrometric and their sedimentation velocities are low resulting in aerosol residence times of months [16]. Volcanic eruptions represent the strongest source of variability in stratospheric aerosol as they can inject substantial amounts of SO_2 directly into the UTLS as well as ash particles for some events [17, 18].

In addition to the sulphate population, aerosols in the UTLS contains fractions of other particle types, i.e. organic particles, a smaller proportion of black carbon and some extraterrestrial material as derived from in situ airborne observations using mass spectrometry [19, 20], single-particle soot photometry [21] or aerosol sample collection/impaction with subsequent composition analysis in the laboratory [22, 23]. The increasing occurrence of wildfires in the warming climate is an important source of injection of black carbons and organic particles in the UTLS [24, 25]. Together with sulphates and organics, the presence of nitrates, ammonium and mineral dust has been reported in the UTLS above the polluted Asian region during summer monsoon by model simulations [26, 27] with possible subsequent influence on the northern hemisphere aerosol content [28]. However, recent aircraft and balloon chemical composition measurements indicate the dominance of secondary aerosols such as nitrate, organics and sulfate with a degree of oxidation increasing with altitudes [29, 30]. It remains uncertain if these particles are in an internal or external mixture with the sulfuric acid droplets though [19] suggest rather internal mixtures of sulfate and carbonaceous material. During their transport, their composition of organic aerosols is transformed by oxidation, cloud processing and wet/dry deposition [31-33]. However, the detailed processes involved in the formation of organic aerosols, the chemical composition of the organic fraction and its potential impacts on the chemical and optical properties of UTLS aerosols are still unclear. Most of the observations of OA have been obtained in the troposphere (or in laboratory experiments excluding thermodynamical and chemical conditions of the UTLS). Chemical composition, air mass residence times and UV flux between the lower troposphere and the UTLS are too different to apply directly the results obtained for tropospheric OA. Available sampling techniques in the UTLS are limited due to the restricted number of research platforms and instruments capable of sampling at these altitudes. Therefore, it is particularly important to improve the knowledge about the organic aerosols in the UTLS in order to identify the sources and processes leading to aerosol presence and production there.

In this study, we analyze gas and aerosol samples collected on balloon-borne filters from the lower troposphere to the stratosphere at mid-latitudes for the first time, to our knowledge, with altitude segregation and subsequent information on the chemical organic composition derived from high resolution mass spectrometry (Orbitrap, Q-Exactive, Thermo Scientific). The major aim of this study is to present the new method and gain insight into the differences between the troposphere and the stratosphere in term of organic chemicals composition. Chemical analysis may help to better understand the sources and processes controlling the composition of the UTLS region.

2. Experimental

2.1 Materials and methods

2.1.1 Sampler description

The CHEM Filter Sampler (referred as Sampler herein below) is a system that collects particles on several filters for time-resolved sampling[34]. The system was adapted for balloon flight applications using a micro-controller connected via serial communication and an InterMet radiosonde that collects weather parameters (Pressure, Temperature, Relative Humidity) as well as Global Position System locations (Lon, Lat, Alt). The

sampler is composed of eight filter cartridges that hold the individual filters (Fig S1-a). The eight channels allow to perform time-resolved and/or altitude-based sampling. An external rotating disk with permanent magnets interacts with internal valve magnets so that only one valve opens at a given time depending on altitudes. The rotating disk is located downstream from the filters. The sampled flow rate is measured by a laminar flow element on the inlet (Fig S1-b). The sampled flow is controlled by modulating the speed of the integrated vacuum pump. The sampler is controlled based on the pressure measured by the Imet radiosonde. Once started, the unit automatically exposes each filter to the sampled flow within a given atmospheric layer between a lower and an upper pressure bounds. During position change, the pump is turned off. The aerosol sampler was cleaned thoroughly with isopropyl alcohol before each flight.

2.1.2 Sampler preparation

Activated carbon cloth (ACC) referenced CT27 (Mast CARBON UK) prepared from a viscose precursor was used as an adsorbent to collect the volatile organic compounds (VOCs) and organic aerosols (OAs) present in the atmosphere[35, 36]. The nanotexture, porosity and chemical functionalities of CT27 have been fully characterized in a previous work[37]. These activated carbon materials have a highly developed specific surface and are used in air pollution control applications. Their effectiveness is recognized for the filtration of VOCs and the trapping of molecules. In the form of fabrics, these materials are self-standing filters easy to handle and present the advantage of not releasing any fine particles and dusts. The fabrics used are composed of carbon fibers with an average diameter of 1 µm with a range of porosity covering several orders of magnitude (micropores < 2 nm, mesopores between 2 and 50 nm, and macropores with diameter > 50nm). The porosity is directly accessible all along the fibers allowing a quick diffusion of molecules within the porosity followed by physical or chemical adsorption on adsorption sites and capillary condensation in the micropores. These fibers were selected for their hydrophilic properties originated from a high oxygen content 3.7 wt % determined by temperature programmed desorption analysis; the oxygen heteroatoms present in the carbon structure being arranged in acidic functionalities. Their nitrogen adsorption isotherm is of type IV showing an hysteresis characteristic of a micro/mesoporous material. The specific surface area was over 1100 m^2/g with a total pore volume of 0.75 cm^3/g, a micropore volume (pores between 0.7 to 2 nm) of 0.43 cm^3/g (N_2 adsorption) and a mesopore volume (pores from 2 to 50 nm) of. CO_2 adsorption showed a high ultramicropore volume (pores below 0.7 nm) of 0.45 cm^3. The pore size distribution determined by applying DFT model on nitrogen adsorption isotherm shows mainly two ranges of pore sizes, around 1.2 and 3.8 nm able to trap small gaseous molecules or oligomers and aerosols respectively. Based on the properties of those filters, we therefore assume that the system can collect gases and aerosols.
Two filters, 1.3 cm in diameter, of this fabric were cut out, superimposed and loaded in each filter cartridge for aerosol and gas collections along the air flow (Fig 1-c). After the flight, filters were placed in individual aluminum foil and named according to their respective positions. To limit chemical transformation, the sample were stored in a desiccator which was swept more than ten times its volume with nitrogen (99.995 % pure) to eliminate all traces of humidity and oxygen. For the flight data presented in this study, the sampler was loaded at ~13h00 and unloaded after recovery near ~19h00. The chemical analyzes were carried out three days after the atmospheric sampling.

2.1.3 Balloon flights (18/01/2022)

On 18 January 2022, 3 balloon flights took place from Reims (France) as part of the Radiosondage des Evenements extremes et des Aerosols de la Stratosphere (REAS) campaign (Dumelie et al., 2022, in prep). The first flight was launched at 9h08 and included a Particle plus Optical Counter (POPC) for which the concentration profiles are shown in Fig. 2. The second flight launched a few minutes later embarked an M20 radiosonde, an electrochemical Concentration Cell and an Aircore sampling system. Vertical profiles of temperature, O_3, and CO mixing ratio are shown in the middle panel of Fig. 2. Finally, a third flight took place at 14h03 with the sampler. The flow rate profile (lpm) colored by position Id (N1 to N5) is shown (Fig. 2, right). The aerosol, trace gases and temperature profiles provide meteorological and chemical information within the layers sampled during the flight. The cold point tropopause (~13km) marks a transition with a positive gradient in aerosol concentration (increase by a factor 10) for all sizes as well as ozone concentration while CO concentration decreases by more than 50%. The transition region between the troposphere and the stratosphere also known as the UTLS region was sampled on position 4 between 9.4-14.9 km. In the free troposphere where aerosol concentration for r>0.15 µm is lower than in the stratosphere was sampled on

position 3. Above the cold point tropopause near 12 km, two distinct regions of the stratosphere exist. Between 12-16 km, higher concentration of ozone is collocated with increased aerosol concentration for larger size (>0.4µm) while the layer above 16 km is marked by an increase of ozone but with smaller aerosols concentration. The region between 12-16 km corresponds to the lowermost stratosphere, an active zone of exchanges with the tropical and mid-latitude troposphere while the lower stratosphere above 16 km is generally influenced by the horizontal and downward motions of the Brewer Dobson circulation [23]. We also note that CO displays behavior changes within the two layers. The upper layer was sampled on position 5 of the sampler and was likely influenced by air masses transported from the tropics.

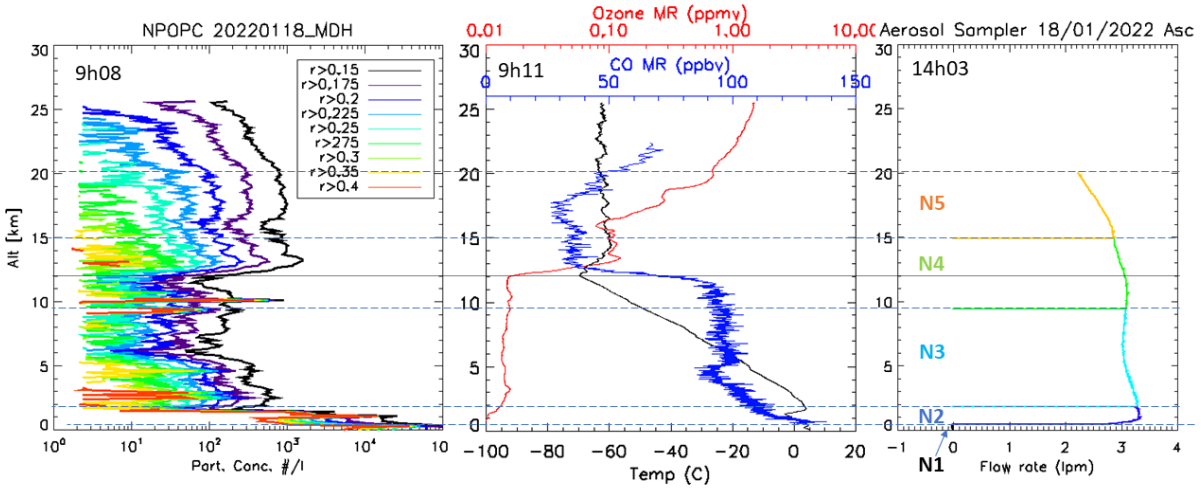

Fig. 2. (Left panel). Particle concentration for 9 size radii between 0.15 µm and 0.4 µm measured by the Particle plus Optical Counter (POPC) on a balloon flight on 18/01/2022 at 9h08 (launch time) from Reims. (middle) Corresponding temperature, ozone and CO profiles measured by an M20 radiosonde, an Electrochemical Concentration Cell (ECC) and Aircore on a second flight which took place a few minutes after. We note that the Aircore retrieved CO was measured during the descent (right). Flow rate on different filter position (N1 to N5) during a third flight with the aerosol sampler launched at 14h03.

The goal of the sampler flight was to collect gas and aerosol samples from distinct atmospheric layers for which differences were highlighted from the POPC observations (Fig.2). The derived layers and corresponding sampling characteristics are described in Table 1. We selected the levels of each layer using an aerosol profile derived from the Compact Optical Backscatter for Aerosol Detection (COBALD) the previous night (Fig.S2). The ozone and aerosol profiles indicate that those layers, in which N4 and N5 were sampled, have likely different origins. Higher ozone values would indicate a tropical origin also associated with volcanic aerosols from La Soufriere eruption which took place in April 2021, i.e., 9 months prior to the balloon flight. The transport of the plume is apparent from the observations of the CALIPSO spaceborne lidar (Fig. S4). At lower levels (9-15 km), the second peak might be associated with residual of smoke from biomass burning which took place during the summer and fall 2021. In the troposphere, the boundary between N2 and N3 was chosen to differentiate aerosols in the planetary boundary layer with a top located near 2 km (very sharp decrease of aerosol concentration) and the free troposphere above.

Table 1. Summary of the filter position number, altitude range, samples time (ST), sampled volume (SV), temperature in Kelvin, atmospheric pressure and number of moles (n) during the balloon flight on 18 January 2022.

Position # (filter No.)	**Altitude range (km)**	**Pump status**	**ST (s)**	**SV (l)**	**T(K)**	**P atm**	**n**
P1 (N1)	Ground-0.5	Off	11714	-3	-	1	-
P2 (N2)	0.5-1.8	On	562	30	273	0.86	1.1525
P3 (N3)	1.8-9.4	On	2659	134	233	0.38	2.665
P4 (N4)	9.4-14.9	On	1629	81	208	0.08	0.38
P5 (N5)	14.9-20	On	1525	66	213	0.02	0.0756

2.1.3 Sample analysis

Samples collected on ACCs were analyzed by high-resolution mass spectrometry (Orbitrap Q-Exactive, Thermo Scientific). The IonMax HESI II source has been modified by soldering a gold foil onto the corona needle. The filters were placed on this new gold support using mounting brackets. We used desorption electrospray ionization (DESI), a soft ionization technique, to analyze the chemicals present on the filters in their native state [38, 39]. With this mode of ionization, the ionic intensities do not directly reflect the concentrations of the chemicals present on the filter. This method of analysis is extremely sensitive (low femtograms per squared millimeter) [40] but, the present data is therefore only of a qualitative nature. Figure S3 presented in the Supplements shows the assembly used in this work.

Analyses were performed by direct instillation of toluene (flow injection analyses - FIA) for chemical ionization A Heated electrospray ionization source (HESI) was used. The FIA settings for HESI ionization were: sheath gas 20 arbitrary units (a.u.), auxiliary gas flow 0, vaporizer temperature 120°C, capillary temperature 280°C, spray voltage 3 kV, flow injection of 6µL/min recorded for 1 min for data averaging. The Orbitrap® Q-Exactive from Thermo Scientific has a mass resolution of 140,000 and mass accuracy <0.5 ppm RMS. Mass calibrations in positive and negative HESI were performed using Pierce™ calibration mixtures (Thermo Scientific). The maximum ion injection time was set to 200 ms with an automatic gain control of 10^6. For each sample, the faces exposed to the atmosphere, were analyzed using positive and negative ionization modes. All samples were analyzed three times three mass ranges (m/z 50-750, 200-1000, and 500-2000). The use of different mass ranges aims to correct for the decrease in trapping efficiency at higher masses. A more detailed description of these technical aspects is available in a recent review[41]. Using several mass ranges allows detecting simple molecules, oligomers but also nano aerosols of a few dozen nanometers in diameter. For larger aerosols, only the parts extracted by desorption with m/z< 2000 will be detected[42]. In mass spectrometry, m/z close to 2000 Da correspond to chemicals up to 0.02 um in size. We observed a gradual growth of the size of VOCs towards that of aerosols (POPC). The DESI sensitivity which allows the measurement of a few thousandths of a mole, is suitable for the mole concentrations observed during this flight (Tab.1).

2.2 Data Processing

High resolution mass spectrometry generates a large amount of data that is easier to interpret with visualization tools [43-46]. In this study, we used double bond equivalent (DBE), van Krevelen diagrams, carbon oxidation state (OSc), and degree of unsaturation as a function of m/z for these representations. Molecules with carbon, hydrogen, oxygen, nitrogen, and sulfur atoms were sought. Molecular formula assignments were made with a maximum mass deviation of 3 ppm and an intensity greater than 10^3. Molecular formula with an intensity lower than $5.0x10^3$ and detected only once out of three analyzes were not retained. The DBE represents the sum of the number of unsaturation (double bond and ring) present in a chemical compound [43]. Decreasing the number of hydrogen atoms increases its value. DBE is defined as:

$$DBE = 1+c -h/2+n/2$$

(c= number of carbon atoms; h = number of hydrogen atoms; n= number of nitrogen atoms)

for elemental composition $C_cH_hN_nO_oS_s$ where only divalent sulfur is considered.

The van Krevelen diagram [47, 48] shows the evolution of the H/C ratio as a function of O/C for a set of identified chemical formulas. In a complex organic mixture, this type of representation allows the identification of classes of compounds such as aliphatics, aromatics or highly oxidized compounds.
The carbon oxidation state (OSc) measures the degree of oxidation of organic species (alcohols, aldehydes, carboxylic acids, esters, ethers and ketones, but not peroxides) [49-51]. It is defined by the following equation:

$$OSc \approx 2O/C - H/C$$

The percentage of unsaturation [52] was calculated by dividing the DBE number for each chemical formula identified by the number of single bonds in a saturated hydrocarbon having the same number of carbon atoms (CN). All molecular ratios, DBE numbers, and chemical formulas presented in this article refer to neutral molecules.

Unsaturation % = DBE/ (3* CN +1) *100

3. Results and discussion

3.1 Obtained main chemical formulas and classification

The data processing carried out on all six filters (Virgin + 1-5) gave six sets of chemical formulas. Given the data filtering criteria presented previously, we searched for $C_cH_hN_nO_oS_s$ molecules in positive and negative modes.

For the chemical formulas identified as containing sulfur, only the presence of H_2SO_4 could be verified on the filters 1 to 5 (negative mode). This detection is expected since sulfur is a major gas emitted in the troposphere from anthropogenic activities (in the form of SO_2) and that sulfuric acid droplets are ubiquitous in the UTLS and the stratosphere via anthropogenic (SO_2, DMS, OCS) and volcanic (SO_2) sources. The stratosphere was likely influenced by La Soufriere eruption as seen by an increase of aerosol concentration from the OPC (Fig.2) which likely led to reinforce the H_2SO_4 signature observed with the Orbitrap. For the other chemical formulas, the isotopic analysis did not confirm their presence, either because of too low intensity of ^{32}S (if ^{32}S is$<10^5$ then $^{34}S<10^3$), or by the absence of the mass containing the ^{34}S isotope. Its detection on the filters is a first indication of the quality of the samples and the measurements by mass spectrometry.

We also searched in filter 1 for potential contamination and identified a series of fluorinated compounds characteristic of PolyTetraFluoroEthylene (PTFE). This contamination was also identified on filters 2 to 5 and coming from PTFE filters used during previous samplings. No other contamination could be identified.

Among all the other chemical formulas detected, we restricted the study to VOCs and OAs composed only of carbon, hydrogen and oxygen which constitute the majority of VOCs and OAs present in the atmosphere, i.e, hydrocarbons, oxygenated VOC, OAs, and polycyclic aromatic hydrocarbons, (PAHs)[53].

In the first part of this study, we compared the results obtained for the different faces of the filters for the same sampling zone (face exposed to the atmosphere – AF; face facing each other– FF; and the face oriented to the diaphragm pump - MF). An average reduction of 20% in intensities is observed and consequently a reduction in the chemical formulas identified from AF to FF and FF to MF. Therefore, we used the data from the faces exposed to the atmosphere for comparison.

Under these conditions, for the six filters, we identified a total of 6589 chemical formulas. In order to process these large data sets, we used graphical tools previously described [43]. We used the van Krevelen representation and gave for each filter the number of chemical formulas identified (Fig. 4). This allows identifying families of chemical compounds [54] ; here it highlights differences in oxidation (O/C ratio) and unsaturation (H/C) specific to the samples collected on each filter.

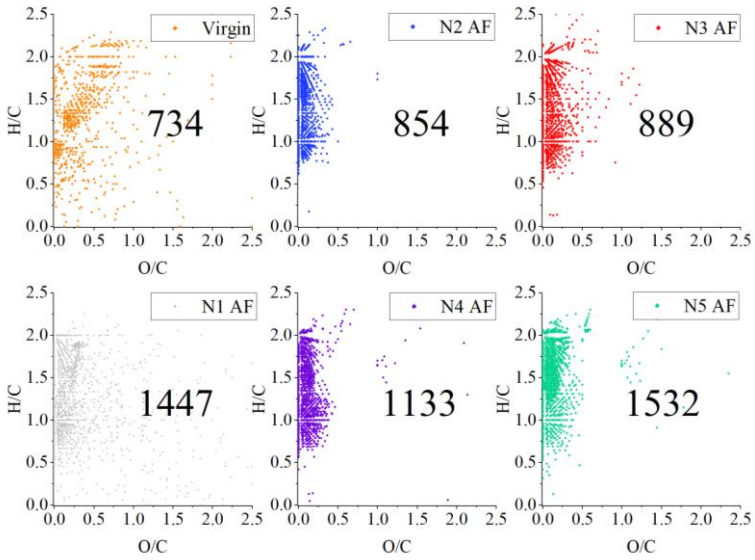

Fig. 4. van Krevelen diagrams for the six filters

We correlated the six lists of $C_cH_hO_o$ chemical formulas identified on filters 2-5 to the physical parameters of the flight (atmospheric pressure and gas flow). It appears that the amount of gas flowing through the filters had little impact on the number of chemical formulas detected, unlike the decrease in pressure which, with altitude, enabled adsorption to be activated on the surfaces of the filters.
In order to highlight the possible logical relationship between these filters, a Venn diagram was built (Fig. 5).

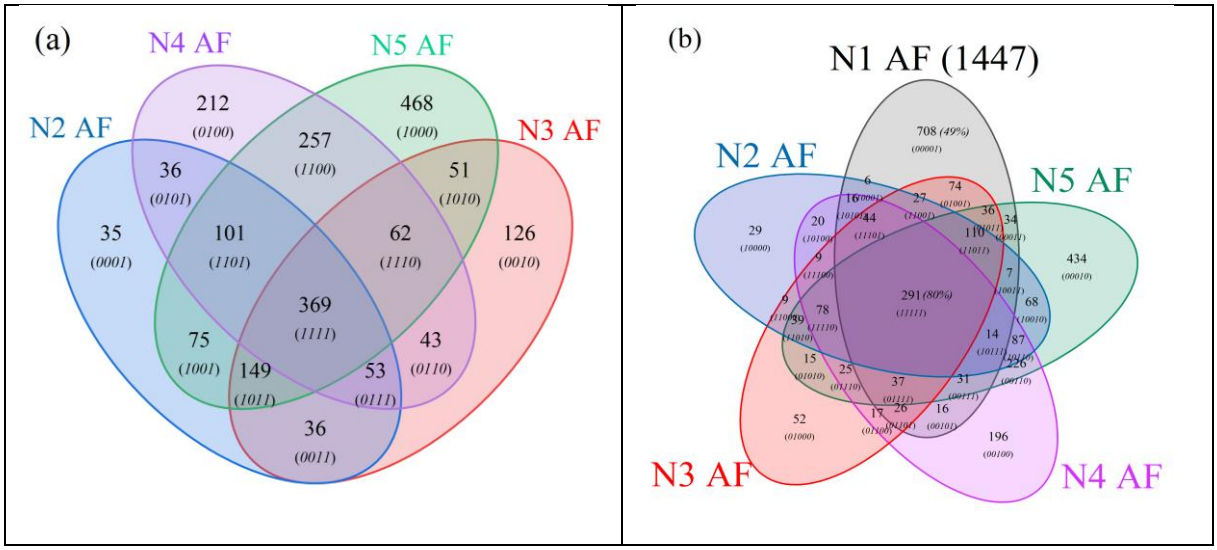

Fig. 5. (a) Venn diagram showing common chemical formulas detected in samples 2-5 AF, (b) Venn diagram showing common chemical formulas detected in samples N2-N5 AF compared to N1.

This diagram shows (Fig. 5a) 15 sets (0001-1111) which could reflect atmospheric similitudes between the different sampling zones. We defined four groups of data according to the following criteria. The first group contains only the data of the set (1111) common to the four filters. These 369 chemical formulas represent 30% of the total population identified for the four filters. Among the 369 common species, some might represent some levels of contamination but could also be indicative of common species throughout the atmosphere. The second group consist of sets common to two or three neighboring sampling areas. For example, these are the sets common to filters 2 and 3, or 3, 4 and 5. The third group consists of the four sets specific to a sampling zone: (0001), (0010), (0100), and (1000). Finally, the last group contains the other sets of which at least one of the sampling zones is distant, i.e., not contiguous (e.g., 2-4; 2-3-5). This last group represents only 20% of all chemical formulas. These distant groups that nevertheless share chemical formulas have not been studied. They may be the result of exchanges between the different layers. However, the absence of information on such exchanges has not allowed to confirm this hypothesis [25, 55]. The constitution of these four groups allowed us to make the new observations described in the next paragraphs.

3.2 Origin of the group (1111) common to all four filters

It is important to determine the origin of this group in order to know if these chemical formulas can correspond to those detected during this flight. This group can have different origins such as contamination by the media used, residual adsorption inherent to the exposure of these filters before and after the flight or chemical adsorption related to the flight. To verify the first hypothesis, we compared the data from reference filters, i.e., N1 et Virgin.
The N1 filter underwent the same theft as the other four filters. However, it was not subjected to a flow of gas, but simply to the pressure variations due to the theft. Adsorption was therefore reduced.
For the Virgin filter, which was not flown, (no gas flow or pressure variation), the percentage of common chemical formulas with all four filters (2-5) is only 10%. Common chemical formulas set with space (1111) is reduced to 1%. In order to complete this comparison, we have represented the Virgin reference and the group (1111) using a 3D diagram including the DBE number in addition to a van Krevelen graph (Fig. 6).

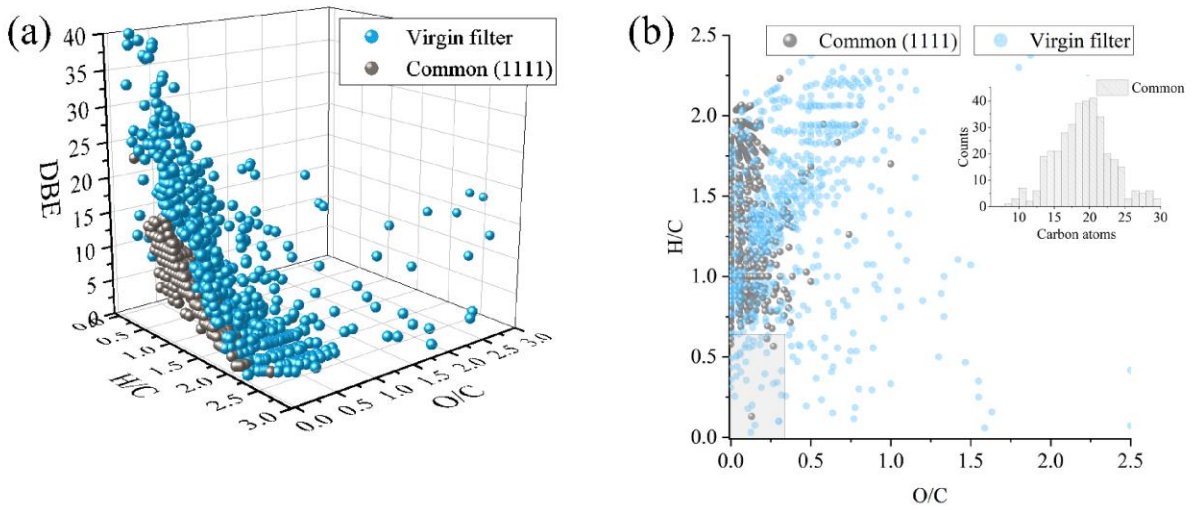

Fig. 6. Comparison of the two groups (1111) and Virgin: (a) van Krevelen graph with DBE number, (b) without DBE number and with PAH and oxy-PAHs chemical fingerprint (grey area); inset plot: distribution of the carbon number (1111)

This representation has the advantage (i) of avoiding the superposition of points linked to the van Krevelen representation and (ii) of providing new chemical information, i.e., unsaturation. The differences between these two groups are clearly visible in terms of the number of unsaturation and the O/C atomic ratios. We thus observe on the Virgin reference (Fig 6a), a larger number of chemical formulas with a DBE > 15 compared to the group (1111). The chemical formulas with a DBE > 15 are mainly positioned in the gray zone of the Van Krevelen graph (Fig. 6b). This chemical character (0<H/C<0.75 and O/C<0.35) corresponds to PAHs and oxy-PAHs. This consistent with the chemical composition of the graphite planes present in the filters used. The Virgin filter was not exposed to the pressure variations that occurred during the flight and that favored a uniform adsorption on the surfaces. Finally, the group (1111) does not present, with some exceptions, points in common with the gray area. We can then conclude that the existence of this group (1111) is indeed the result of the flight conditions, without excluding at this stage a contamination before and/or after the flight.

For residual adsorption inherent to the exposure of these filters before and after the flight (second hypothesis), one notes that the identified chemical formulas with dispersed low mass (86% in the range 200 to 340 m/z) and CN centered on 19 (Fig. 6b). Figure S5 shows the central position of this group (1111) among all identified chemical formulas (a) and those specific to each filter (b). Figure S5c shows the chemical formulas specific to each filter without the set (1111). Moreover, we note, that the percentage of unsaturation of the group (1111), in the range 5 to 27%, can result from a wide range of chemical reactions (addition, fragmentation, oligomerization, etc.). One notes that this set fits both in a chemical continuity (e.g. decrease of unsaturation with the increase of m/z), and on the other hand that in the absence of these data, no other chemical formula detected on another filter maintains this continuity. In conclusion, the graphs of Figure 6 show a chemical evolution of the formulas indicating the presence of a common data set. It therefore seems unlikely, given these observations, that such large contaminations would fit so coherently into a remaining chemical set. Without excluding a punctual contamination, the set (1111) can be identified as a common set of chemical formulas present in the atmosphere.

It should be noted that apart from the sampling phases, the filters are isolated and only undergo pressure variations during the path of the balloon flight. This pressure variation induces adsorption without air flow. This passive adsorption can be observed principally on the N1 filter which has undergone the longest passive exposure, i.e., without pump generated flow. On N1, this passive adsorption is characterized by 51% similarity with the totality of the identified chemical formulas and 80% with the set (1111) present along the whole flight (Fig. 5(b)).

3.3 Molecular formulas specific to sampling areas

We compared the chemical formulas detected specifically in each sampling area: N2-AF (0001), N3-AF(0010), N4-AF (0100), and N5-AF(1000). The properties of these chemical formulas were plotted in a Van Krevelen diagram with an extra dimension assigned to unsaturation (DBE). In this type of representation,

the nature of the oxidation (formation of alcohols, carbonyls, unsaturation, etc.) is better described thanks to the inclusion of the DBE parameter (Fig.7-b). To complete these analyzes of the properties of chemical molecules, we have added for each filter the distribution of the carbon number.

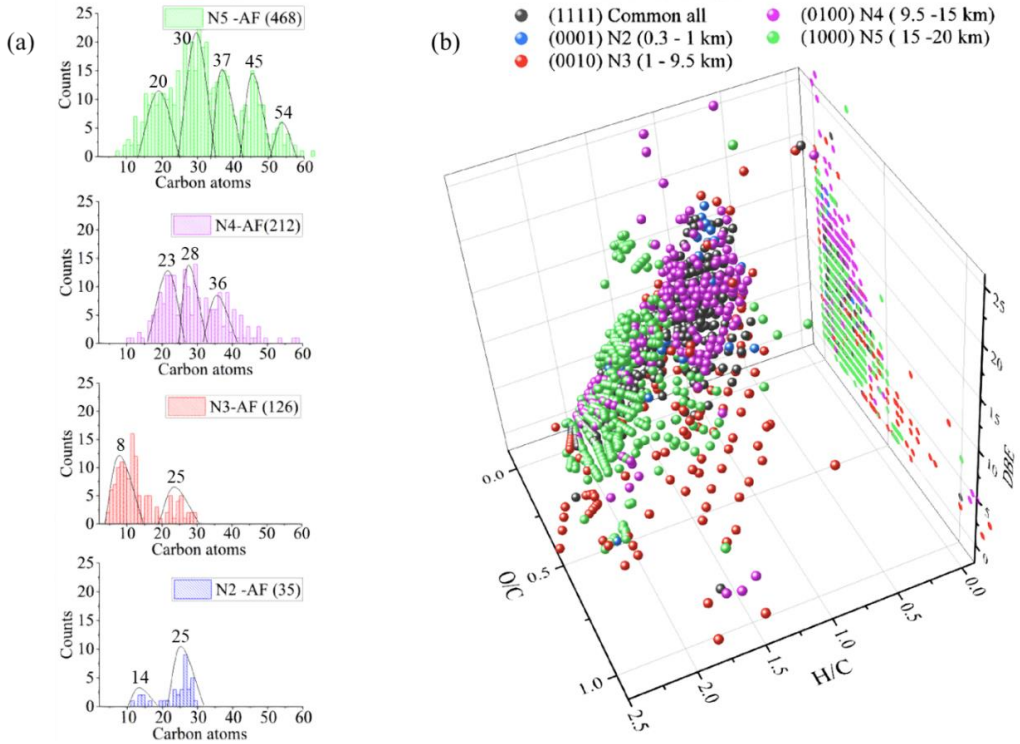

Fig. 7. (a) Carbon number distributions for filters 2 to 5; (b) Van Krevelen graph with DBE number.

We observe on this graph a specific fingerprint of each sampling zone characterized by a centered dispersion of the chemical formulas, the oxidation level, and the amount of unsaturation. These results are correlated with the carbon number (Fig. 7a) and all of these data are particularly significant for filters 3, 4 and 5. For filter 2, the low number of chemical formulas specific to this filter and the dispersion of chemical formulas in this space limits the interpretation of the data. One should note that filter 2 was the one which was the less exposed to air flow between 0.5-1.8 km.

For filter 3, one can observe a more important oxidation with a distribution centered on O/C = 0.5, unlike filters 4 and 5 showing a distribution centered on O/C=0.25 (Fig. 4). The distribution of carbon number is bimodal, but it is difficult to specify whether this observation is part of a process of fragmentation or growth. It is nevertheless observed that the DBE number increases with the length of the carbon number (CN = 10 to CN= 25).

On filter 4, all the chemical formulas with distribution centered on O/C=0.25 and with an average DBE of 12 show unsaturation not linked to the formation of ketones or aldehydes. Similar to filter 3, the growth of the molecules naturally increases this DBE number without significantly modifying the O/C ratio. This growth gives, here too, a multimodal distribution of the carbon number (CN = 23, 28 and 35) and could be assimilated to oligomerization.

On filter 5, the distribution of chemical formulas is centered on O/C = 0.25, with a strong reduction of the DBE number (centered on 5), compared to filter 4. This reduction of unsaturation occurs in parallel with fragmentation /growth and a multimodal distribution of carbon number (CN = 20, 30, 37, 45, and 54). It also occurs in an environment where HO_x and $O(^1D)$ radicals, abundant in the stratosphere, react with unsaturated species. The reduction in the DBE number could result from a breaking of double bonds after addition. At the same time, we observe a strong increase in the number of molecules with an O/C ratio close to 0.25 (2 times higher than the distribution observed on filter 4), which corresponds to an increase in oxidation. (Fig S6). This decrease in unsaturation may explain this wide distribution of CN. More generally, if we observe an effect of atmospheric pressure on adsorption (i.e., the number of adsorbed chemicals), other variations, such as ozone concentration, concentration of oxygen atoms and ionizing radiation (UV) depending on altitude could affect products distribution. Thus, for filter 5, the relatively low pressure (leading to lower reaction kinetics) and the presence of UV radiations could explain the degradation of unsaturated chemicals and an increasing number of oxidized molecules. This type of oxidation would have no significant impact on

the O/C ratio. The OSc graph of Figure 8 offers another visualization of the results and highlights the particularities of each sample. There, we observe a clear oxidation in the low CN range of the N3 filter, much more visible than on filter 2. There is also a strong increase of the CN between the N4 and N5 filters with significant evolution of OSc. There, the group of chemical formulas (1111) is again integrated into a continuum between the different samples.

It is difficult to connect the evolution of chemicals' size with aerosols radii observed by POPC. However, our HRMS observations show that the size the evolution of chemicals' size follows the trend observed by POPC across the atmospheric layers.

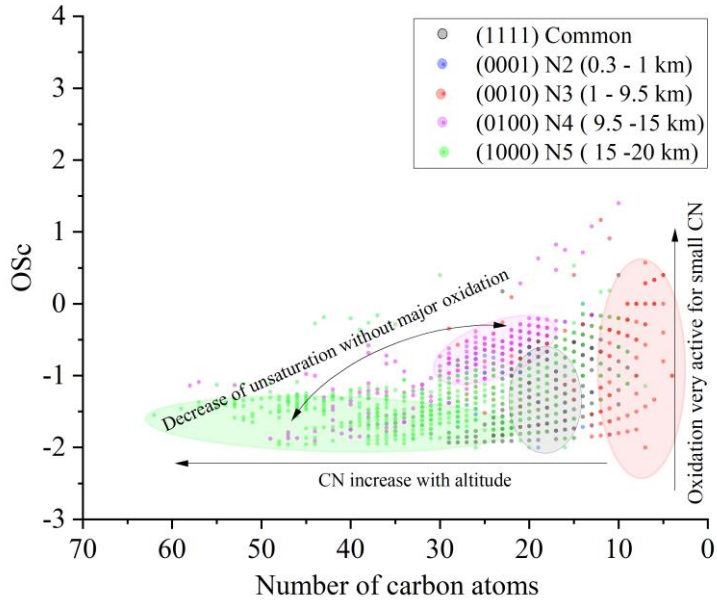

Fig. 8. OSc vs. number of carbon atoms presented for samples N2 to N5. The ellipses show the preferential zones of the different filters.

The data in general, and more particularly on filter 5, do not allow to specify if this increase in the number of carbon atoms is linked to an aging phenomenon.

3.4 Flux between sampled neighbor areas

The sampling zones were defined based on aerosol concentration and backscatter properties from the troposphere to the stratosphere determined during a flight on the previous day. These boundaries are somewhat arbitrary and consecutive samples likely share chemical molecules through exchanges and transport. Table 2 shows how these exchanges evolve between the different samples. These exchanges are analyzed using the number of chemical formulas contained in the common sets. In addition to the number of common chemical formulas, we have expressed this value as a percentage with respect to each of the layers. There are many common species between these layers, greater than 50%, which nevertheless leave room for the particularities observed for each filter, i.e., (0001), (0010), (0100), and (1000).

Table 2. common species at the interfaces of the sampling areas

Interface N2-N3	Interface N3-N4	Interface N4-N5
607 (N2-71%; N3-68%)	527 (N3-59%, N4-46%)	789 (N4-69%, N5-51%)

3.5 Link between distant areas sampled

Fluxes of organic matter between atmospheric layers are poorly documented. Nevertheless, recent works have shown that the ejections of organic matter (e.g. during gigantic fires)[25, 56, 57] or mineral matter (e.g.

during volcanic eruptions) [58] could reach altitudes above 30 km. The distribution of these materials as a function of altitude and the resulting exchanges between atmospheric layers as well as the chemical evolution of carbonaceous matter along its transport, remains to be studied using chemistry-transport models. Our analyzes show common chemical formulas in non-consecutive layers (e.g., sets (0101), (1001), and (1010)). The number of these chemical formulas remains small compared to the total 2073 chemical formulas identified on the filters (2-5). The occasional presence of chemical formulas common to distant layers remain unexplained at this stage of the study, but although the number is small, it is large enough not to be considered as an experimental error.

4 Matching of the identified chemical formulas with the literature

Stratospheric levels corresponding to filter 5 are shown to be impacted by air masses transported from the tropical lower stratosphere (Fig. S2) pointing at a tropical origin of the sources of the detected carbonaceous molecules. O/C ratios in the UTLS have been occasionally reported in the literature and have shown values of 0.18-0.2 [59][23] matching our results obtained for filters 4 and 5. This organic signature is expected to stem from organic volatiles and primary aerosols from the troposphere [23], mostly from the tropical latitudes [19, 20]. However, our method focusses on heavy molecules whereas reported studies may integrate a wider spectrum of organic species and also much large aerosols. Moreover, one should keep in mind that O/C values could depend on the location and season corresponding to various influences of overlying stratospheric layers as controlled by the BD circulation. Wildfires with subsequent injection to stratospheric levels are expected to alter the O/C ratio in this region. However, our values for UTLS levels corresponding to filter 4, possibly impacted by past fire events, appear well below 0.5-1, typically reported for young biomass burning plumes [60, 61]. The measured O/C here could be linked to chemical aging processes all along smoke transport.

The small quantities of materials adsorbed on the filters (2-4) did not allow the use of High Performance Liquid Chromatography (HPLC) for a possible identification of the chemical compounds present. Nevertheless, in the hypothesis of an origin linked to injections from wildfires in Northern America, regularly observed in summer and fall over the past few years, we studied the similarities with chemical composition of biomass burning samples presented in the literature. This comparison remains partial, because it was carried out using chemical formulas and does not consider the phenomena of aging or dilution. Nevertheless, it constitutes a necessary step for a better understanding of the evolution of biomass burning plumes in the atmosphere. For this screening, we selected three studies dealing with biomass burning and containing chemical compounds data. Details on these studies are given in Table 3.

Table 3. References and characteristics of biomass burning studies with percentage of similarity with identified chemical formulas in our study.

Bibliographic reference	Samples	Fuels	Instrument (see supplementary)	Chemical formulae	Percentage similarity
Smith et al. [52]	Laboratory	Biofuel	LTQ-Orbitrap	73	60%
Gilman et al. [62]	Laboratory	Biofuels	GC, PTR, PIT, CIMS, FTIR	65	36%
Hatch et al. [63]	Laboratory Prescribed fires	Biofuels	GC-ToF	15	0%

For each study, a Venn diagram was built and presented in the Supplements (Figures S7-S9). For the three studies considered, only the chemical formulas were considered. For example, the study by Hatch et al. reported 135 chemical compounds with numerous isomers which, in the end gave, 15 chemical formulas. In this case, the lack of similarity with the filter samples can be explained by this low sampling targeted on terpenes with a very low dispersion in number of carbons (mainly between 9 and 12 carbon atoms). For the other two studies, the similarities are significant and support the hypothesis that biomass burning products could have been collected on filters in the present study. The data from these two studies also indicate the existence of a common set of chemical formulas observed at different altitudes. We have 22% and 9% of the chemical formulas identical to the set (1111) for the work of Smith et al. and that of Gilman et al., respectively. Levoglucosan, considered to be the most important and stable marker of biomass burning [64]

is present in the study of. Smith et al. However, due to its estimated time life of 8 days in the atmosphere, it could not be observed in our samples, as could be expected.

5 Conclusion and perspectives

The results of several flights are presented. A range of instruments and techniques were used. A Particle plus Optical Counter, an M20 radiosonde, an electrochemical Concentration Cell, an Aircore sampling system, and a new sampler equipped with carbon filters were used. We collected atmospheric samples on carbon filters through 4 atmospheric layers between 0.8 km to 20 km to separate different source regions. They were analyzed by DESI coupled to high-resolution mass spectrometry.
The samples show 30% common chemical formulas. However, a non-negligible, proportion of chemical formulas are only present on a specific sample (e.g. 10% for the free troposphere on N3 and 35% for the stratosphere on N5) reflecting different sources, chemical processes or/and chemical evolution of the organic matter from the troposphere to the lower stratosphere.

The main results of the chemical analysis show:

i) an increase of the carbon chains from the troposphere to the stratosphere
ii) In the stratosphere, the samples collected show a reduction in unsaturation compared to those collected below (UTLS, sample 4)
iii) the oxidation of organic compounds measured by the O/C ratio remains stable across the layers corresponding to the UTLS and the stratosphere
iv) The number of oxidized compounds increase with altitude

Above 15 km, unsaturated organic compounds are strongly influenced by UV light absorption [Ref], which causes unsaturation breakdown and may also explain the multimodal carbon distribution associated with molecular fragmentation/growth. Despite the increase of ozone concentration, at this altitude, the oxidation of organic compounds measured by the O/C ratio does not increase unlike the number of oxidized compounds, which increases. The fragmentation, possible outcome of the decrease of unsaturation, can explain the observed simultaneous phenomena.

While quasi-coincident aerosol number concentration and size measurements collected with an optical particle counter might be related to the chemical analysis shown here, the sizes of particle measured, a few nanometers with the sampler and more than 300 nm with the optical particle counter make the comparison difficult. Nevertheless, it is not unrealistic to assume that the source regions have produced specific aerosols/molecules that were encountered by both instruments but the connections between both remain challenging to assess.

Ozone and aerosol profiles obtained a few hours before the sampler flight shows that sample 5 was likely influenced by air masses from the tropics associated with enhanced O_3 and aerosols likely influenced by La Soufriere eruption which took place 9 months prior to the flights. At such levels, satellite observations point at air mass origins from tropical latitudes where the higher quantities of organic material have been reported in the literature [19, 20]. It is expected that carbonaceous compounds can remain for months in the stratospheric aerosol particles [19].
The origin of the organic compounds we have detected is still to be determined especially in the UTLS and the stratosphere (e.g. Asian pollution transported upward by cloud convection and then distributed to the northern hemisphere, seasonal fires in South America and Africa). The way combustion products emitted from anthropogenic emissions and natural wildfires evolve, sustain breakdown, results in unsaturated organics and organic radicals, recombine to result in a spectrum of products under varying pressure, temperature, humidity and solar flux all along their transport from the source regions is not clear.

At this stage, although efforts have been made to compute chemistry of secondary organic aerosols and particulate organic matter from the surface to the stratosphere [27], no chemistry-transport model is able to comprehensively simulate the various sources, content and chemical evolution of the organic matter for the heavy molecules we have pointed out in our study.

An important question is whether or not our results are reproducible and correspond to a snapshot of the

atmosphere state or point at a steady feature. Further investigations at other seasons and latitudes, in period non-impacted by volcanic and fire plumes would be necessary to address this question.

Author statements

Roland BENOIT, Conceptualization, sampling, Methodology,Writing the original draft, review & editing, Formal analysis, Supervision.
Hazel Vernier: Writing – review & editing; Investigation; Methodology; Validation
Jean-Paul Vernier: Writing – review & editing; Investigation; Methodology; Validation
Lilian Joly: Writing – review & editing Investigation; Methodology; Validation
Nicolas Dumelié: Writing – review & editing, Investigation; Methodology; Validation
Frank Wienhold: Writing – review & editing, Methodology; Validation
Cyril Crevoisier: Writing – review & editing, Methodology; Validation
Sandrine Delpeux: Writing – review & editing, Filters preparation
Philippe Dagaut: Writing – review & editing
Gwenaël Berthet: Writing – review & editing; Investigation; Methodology; Validation; Funding acquisition; Supervision.

Declaration of competing interest

The authors declare that they have no known competing financial interests or personal relationships that could have appeared to influence the work reported in this paper.

Acknowledgements

JPV thanks the STUDIUM Smart Loire Valley Programme for granting a visiting researcher award at the LPC2E laboratory. The authors gratefully acknowledge funding from the Labex Voltaire (ANR-10-LABX-100-01), support from the NASA Roses Upper Atmospheric Composition Observation program for the balloon flights, support through the HEMERA infrastructure via the European Union's Horizon 2020 research and Innovation program (grant N°730970).
We thank Johnny Mau and Amit Pandit for their technical supports in the payload preparations as well as Marie Angot and Delphine Combaz for the ozone sonde and Aircore preparation. Fred Brechtel for his assistance in operating the aerosol sampler. We are grateful to Francois Bernard, Michel Chartier, Patrick Jacquet, Gilles Chalumeau, and Claude Robert from LPC2E for technical help and fruitful discussions.

Acronyms:

LTQ-Orbitrap: linear trap quadrupole Orbitrap; GC: gas chromatography; PTR: Proton-transfer-reaction; PIT: Proton transfer ion; CIMS: Chemical Ionization Mass Spectroscopy; FTIR: Fourier-transform infrared spectroscopy; GC-ToF: Gas chromatography coupled to time-of-flight mass spectrometry

References

1. Ramanathan, V., et al., *Aerosols, climate, and the hydrological cycle.* Science, 2001. **294**(5549): p. 2119-24.
2. Chin, M., et al., *Intercontinental transport of pollution and dust aerosols: implications for regional air quality.* Atmos. Chem. Phys., 2007. **7**(21): p. 5501-5517.
3. Solomon, S., *Stratospheric ozone depletion: A review of concepts and history*. Reviews of Geophysics, 1999. **37**(3): p. 275-316.
4. Pörtner, H.-O., Roberts, D.C., Tignor, M., Poloczanska, E.S., Mintenbeck, K., Alegría, A., Craig, M., Langsdorf, S., Löschke, S., Möller, V., Okem, A., Rama, B., *Climate Change 2022, Impacts, Adaptation and Vulnerability.* IPCC, WGII Sixth Assessment Report, 2022. **Cambridge University Press.**
5. Zhang, Q., et al., *Ubiquity and dominance of oxygenated species in organic aerosols in anthropogenically-influenced Northern Hemisphere midlatitudes.* Geophys. Res. Lett., 2007. **34**(13): p. L13801.
6. Hallquist, M., et al., *The formation, properties and impact of secondary organic aerosol: current and emerging issues.* Atmos. Chem. Phys., 2009. **9**(14): p. 5155-5236.
7. Shrivastava, M., et al., *Recent advances in understanding secondary organic aerosol: Implications for global climate forcing.* Reviews of Geophysics, 2017. **55**(2): p. 509-559.
8. Kalberer, M., et al., *Identification of polymers as major components of atmospheric organic aerosols.* Science, 2004. **303**(5664): p. 1659-62.
9. Liggio, J. and S.-M. Li, *Organosulfate formation during the uptake of pinonaldehyde on acidic sulfate aerosols.* Geophysical Research Letters, 2006. **33**(13).
10. Ziemann, P.J. and R. Atkinson, *Kinetics, products, and mechanisms of secondary organic aerosol formation.* Chemical Society Reviews, 2012. **41**(19): p. 6582-6605.
11. Sareen, N., S.G. Moussa, and V.F. McNeill, *Photochemical aging of light-absorbing secondary organic aerosol material.* J Phys Chem A, 2013. **117**(14): p. 2987-96.
12. Kremser, S., et al., *Stratospheric aerosol—Observations, processes, and impact on climate.* Reviews of Geophysics, 2016. **54**(2): p. 278-335.
13. Holton, J.R., et al., *Stratosphere-troposphere exchange.* Reviews of Geophysics, 1995. **33**(4): p. 403-439.
14. Weisenstein, D.K., et al., *A two-dimensional model of sulfur species and aerosols.* Journal of Geophysical Research: Atmospheres, 1997. **102**(D11): p. 13019-13035.
15. Chin, M. and D.D. Davis, *A reanalysis of carbonyl sulfide as a source of stratospheric background sulfur aerosol.* Journal of Geophysical Research: Atmospheres, 1995. **100**(D5): p. 8993-9005.
16. Hamill, P., et al., *The Life Cycle of Stratospheric Aerosol Particles.* Bulletin of the American Meteorological Society, 1997. **78**(7): p. 1395-1410.
17. Vernier, J.-P., et al., *Major influence of tropical volcanic eruptions on the stratospheric aerosol layer during the last decade.* Geophysical Research Letters, 2011. **38**(12).
18. Vernier, J.-P., et al., *In situ and space-based observations of the Kelud volcanic plume: The persistence of ash in the lower stratosphere.* Journal of Geophysical Research: Atmospheres, 2016. **121**(18): p. 11,104-11,118.
19. Murphy, D.M., et al., *Carbonaceous material in aerosol particles in the lower stratosphere and tropopause region.* Journal of Geophysical Research: Atmospheres, 2007. **112**(D4).
20. Murphy, D.M., et al., *Observations of the chemical composition of stratospheric aerosol particles.* Quarterly Journal of the Royal Meteorological Society, 2014. **140**(681): p. 1269-1278.
21. Schwarz, J.P., et al., *Single-particle measurements of midlatitude black carbon and light-scattering aerosols from the boundary layer to the lower stratosphere.* Journal of Geophysical Research: Atmospheres, 2006. **111**(D16).
22. Schütze, K., et al., *Sub-micrometer refractory carbonaceous particles in the polar stratosphere.* Atmos. Chem. Phys., 2017. **17**(20): p. 12475-12493.
23. Martinsson, B.G., et al., *Formation and composition of the UTLS aerosol.* npj Climate and Atmospheric Science, 2019. **2**(1): p. 40.
24. Kloss, C., et al., *Transport of the 2017 Canadian wildfire plume to the tropics via the Asian*

monsoon circulation. Atmos. Chem. Phys., 2019. **19**(21): p. 13547-13567.
25. Khaykin, S., et al., *The 2019/20 Australian wildfires generated a persistent smoke-charged vortex rising up to 35 km altitude.* Communications Earth & Environment, 2020. **1**(1): p. 22.
26. Fairlie, T.D., et al., *Estimates of Regional Source Contributions to the Asian Tropopause Aerosol Layer Using a Chemical Transport Model.* Journal of Geophysical Research: Atmospheres, 2020. **125**(4): p. e2019JD031506.
27. Bossolasco, A., et al., *Global modeling studies of composition and decadal trends of the Asian Tropopause Aerosol Layer.* Atmos. Chem. Phys., 2021. **21**(4): p. 2745-2764.
28. Khaykin, S.M., et al., *Variability and evolution of the midlatitude stratospheric aerosol budget from 22 years of ground-based lidar and satellite observations.* Atmos. Chem. Phys., 2017. **17**(3): p. 1829-1845.
29. Appel, O., et al., *Chemical analysis of the Asian Tropopause Aerosol Layer (ATAL) with emphasis on secondary aerosol particles using aircraft based in situ aerosol mass spectrometry.* Atmos. Chem. Phys. Discuss., 2022. **2022**: p. 1-37.
30. Vernier, H., et al., *Exploring the inorganic composition of the Asian Tropopause Aerosol Layer using medium-duration balloon flights.* Atmos. Chem. Phys., 2022. **22**(18): p. 12675-12694.
31. Pöschl, U., *Atmospheric aerosols: composition, transformation, climate and health effects.* Angew. Chem., Int. Ed., 2005. **44**: p. 7520.
32. Jimenez, J.L., et al., *Evolution of organic aerosols in the atmosphere.* Science, 2009. **326**(5959): p. 1525-9.
33. Zhao, Y., A.G. Hallar, and L.R. Mazzoleni, *Atmospheric organic matter in clouds: exact masses and molecular formula identification using ultrahigh-resolution FT-ICR mass spectrometry.* Atmos. Chem. Phys., 2013. **13**(24): p. 12343-12362.
34. Bates, T.S., et al., *Measurements of atmospheric aerosol vertical distributions above Svalbard, Norway, using unmanned aerial systems (UAS).* Atmos. Meas. Tech., 2013. **6**(8): p. 2115-2120.
35. Wang, X., et al., *Key factors and primary modification methods of activated carbon and their application in adsorption of carbon-based gases: A review.* Chemosphere, 2022. **287**: p. 131995.
36. Pui, W.K., R. Yusoff, and M.K. Aroua, *A review on activated carbon adsorption for volatile organic compounds (VOCs).* Reviews in Chemical Engineering, 2019. **35**(5): p. 649-668.
37. Delpeux-Ouldriane, S., et al., *The role played by local pH and pore size distribution in the electrochemical regeneration of carbon fabrics loaded with bentazon.* Carbon, 2015. **94**: p. 816-825.
38. Chan, C.-C., et al., *Desorption Ionization by Charge Exchange (DICE) for Sample Analysis under Ambient Conditions by Mass Spectrometry.* Journal of the American Society for Mass Spectrometry, 2010. **21**(9): p. 1554-1560.
39. Costa, A.B. and R. Graham Cooks, *Simulated splashes: Elucidating the mechanism of desorption electrospray ionization mass spectrometry.* Chemical Physics Letters, 2008. **464**(1): p. 1-8.
40. Yang, S., et al., *Desorption Electrospray Ionization Tandem Mass Spectrometry for Detection of 24 Carcinogenic Aromatic Amines in Textiles.* Analytical Chemistry, 2009. **81**(15): p. 6070-6079.
41. Hecht, E.S., et al., *Fundamentals and Advances of Orbitrap Mass Spectrometry*, in *Encyclopedia of Analytical Chemistry*. 2019. p. 1-40.
42. Marinkovic, N.S., K. Sasaki, and R.R. Adzic, *Determination of Single- and Multi-Component Nanoparticle Sizes by X-ray Absorption Spectroscopy.* Journal of The Electrochemical Society, 2018. **165**(15): p. J3222-J3230.
43. Nozière, B., et al., *The Molecular Identification of Organic Compounds in the Atmosphere: State of the Art and Challenges.* Chemical Reviews, 2015. **115**(10): p. 3919-3983.
44. Wang, X., et al., *Chemical Characteristics of Organic Aerosols in Shanghai: A Study by Ultrahigh-Performance Liquid Chromatography Coupled With Orbitrap Mass Spectrometry.* Journal of Geophysical Research: Atmospheres, 2017. **122**(21): p. 11,703-11,722.
45. Walser, M.L., et al., *High-resolution mass spectrometric analysis of secondary organic aerosol produced by ozonation of limonene.* Physical Chemistry Chemical Physics, 2008. **10**(7): p. 1009-1022.

46. Tu, P., W.A. Hall, and M.V. Johnston, *Characterization of Highly Oxidized Molecules in Fresh and Aged Biogenic Secondary Organic Aerosol.* Analytical Chemistry, 2016. **88**(8): p. 4495-4501.
47. Van Krevelen, D., *Graphical statistical method for the study of structure and reaction processes of coal.* Fuel, 1950. **29**: p. 269.
48. Kim, S., R.W. Kramer, and P.G. Hatcher, *Graphical Method for Analysis of Ultrahigh-Resolution Broadband Mass Spectra of Natural Organic Matter, the Van Krevelen Diagram.* Analytical Chemistry, 2003. **75**(20): p. 5336-5344.
49. Kroll, J.H., et al., *Carbon oxidation state as a metric for describing the chemistry of atmospheric organic aerosol.* Nature Chemistry, 2011. **3**(2): p. 133-139.
50. Bianchi, F., et al., *Highly Oxygenated Organic Molecules (HOM) from Gas-Phase Autoxidation Involving Peroxy Radicals: A Key Contributor to Atmospheric Aerosol.* Chemical Reviews, 2019. **119**(6): p. 3472-3509.
51. Koch, B.P. and T. Dittmar, *From mass to structure: an aromaticity index for high-resolution mass data of natural organic matter.* Rapid Communications in Mass Spectrometry, 2006. **20**(5): p. 926-932.
52. Smith, J.S., A. Laskin, and J. Laskin, *Molecular Characterization of Biomass Burning Aerosols Using High-Resolution Mass Spectrometry.* Analytical Chemistry, 2009. **81**(4): p. 1512-1521.
53. Sindelarova, K., et al., *Global data set of biogenic VOC emissions calculated by the MEGAN model over the last 30 years.* Atmos. Chem. Phys., 2014. **14**(17): p. 9317-9341.
54. Van Krevelen, D.W., *Graphical-statistical method for the study of structure and reaction processes of coal.* Fuel, 1950. **29**: p. 269-284.
55. Lestrelin, H., et al., *Smoke-charged vortices in the stratosphere generated by wildfires and their behaviour in both hemispheres: comparing Australia 2020 to Canada 2017.* Atmos. Chem. Phys., 2021. **21**(9): p. 7113-7134.
56. Peterson, D.A., et al., *Wildfire-driven thunderstorms cause a volcano-like stratospheric injection of smoke.* npj Climate and Atmospheric Science, 2018. **1**(1): p. 30.
57. Hirsch, E. and I. Koren, *Record-breaking aerosol levels explained by smoke injection into the stratosphere.* Science, 2021. **371**(6535): p. 1269-1274.
58. Kloss, C., et al., *Stratospheric aerosol layer perturbation caused by the 2019 Raikoke and Ulawun eruptions and their radiative forcing.* Atmos. Chem. Phys., 2021. **21**(1): p. 535-560.
59. Friberg, J., et al., *Sources of increase in lowermost stratospheric sulphurous and carbonaceous aerosol background concentrations during 1999–2008 derived from CARIBIC flights.* Tellus B: Chemical and Physical Meteorology, 2014. **66**(1): p. 23428.
60. Fang, Z., et al., *Open burning of rice, corn and wheat straws: primary emissions, photochemical aging, and secondary organic aerosol formation.* Atmos. Chem. Phys., 2017. **17**(24): p. 14821-14839.
61. Hodshire, A.L., et al., *Aging Effects on Biomass Burning Aerosol Mass and Composition: A Critical Review of Field and Laboratory Studies.* Environmental Science & Technology, 2019. **53**(17): p. 10007-10022.
62. Gilman, J.B., et al., *Biomass burning emissions and potential air quality impacts of volatile organic compounds and other trace gases from fuels common in the US.* Atmos. Chem. Phys., 2015. **15**(24): p. 13915-13938.
63. Hatch, L.E., et al., *Highly Speciated Measurements of Terpenoids Emitted from Laboratory and Mixed-Conifer Forest Prescribed Fires.* Environmental Science & Technology, 2019. **53**(16): p. 9418-9428.
64. Cao, M., et al., *Seasonal variations and potential sources of biomass burning tracers in particulate matter in Nanjing aerosols during 2017–2018.* Chemosphere, 2022. **303**: p. 135015.